Approach for Establishing Approximate Load Carrying Capacity for Bridges with Unknown Material and Unknown Design Properties

Zach Taylor
Omar Amini
Prof. John W. van de Lindt

Colorado State University
Fort Collins, Colorado

July 2011

Disclaimer

ABSTRACT

There are 16 small to medium simple span bridges in Larimer County that are currently load rated solely based on visual inspections. Most of these bridges are prestressed concrete bridges. The objective of this project is to load rate these bridges using structural analysis with very little to no information available related to their design. Larimer County provided everything available, which essentially was very limited plans and inspection reports for the bridges. The plans lacked details concerning prestress, cross-section dimensions, and material properties. The bridge (prestress concrete) manufacturer does not have records of the bridges built in the 1960's or earlier. Due to these limitations, a basic structural analysis was performed using a program developed for CDOT in 2007 with rating-conservative assumptions in order to determine the capacities of the bridges. The influence of these assumptions on the conclusions is also discussed.

TABLE OF CONTENTS

LIST OF TABLES

LIST OF FIGURES

1. INTRODUCTION

In Larimer County, Colorado, there are a number of county bridges that may not have accurate load ratings because of the lack of blueprints, plans, or specifications. Currently, the load ratings for these bridges are based on visual inspections. The purpose of this project is to systematically develop load ratings for 16 specific bridges through structural analysis as an example of the procedure that may be used in such cases to provide a conservative load rating.

All 16 bridges were constructed between 1935 and 1978, and their spans range from 20 to 73 feet. The bridges are arbitrarily numbered in this study for ease of reference. The bridges in this study numbered 14 and 15 were both originally constructed in 1940 and were reconstructed in 1970 and 1965, respectively. Bridges 2, 5, 13, 14, and 16 currently have posted load limitations of 25 tons.

Fourteen bridges were constructed with prestressed girders and two were constructed with reinforced concrete slabs. The two reinforced concrete bridges are numbered 7 and 15. Bridge 15 was modified with the use of concrete girders that were presumably prestressed, although this is not known with 100% certainty. Basic information of the bridges included in this study is listed in Table 1.1.

Table 1.1 Bridge List

Bridge Number	Year Built	Clr. Span (ft)	Girder Type
1	1966	71.5	Prestressed, precast, T-girder
2	1960	25.8	Prestressed, precast, double T-girder
3	1960	59.0	Prestressed, precast, box girder
4	1965	57.7	Prestressed, precast, double T-girder
5	1963	20.3	Prestressed, precast, double T-girder
6	1960	39.5	Prestressed, precast, double T-girder
7	1935	34.8	Concrete slab
8	1978	73.0	Prestressed, precast, double T-girder
9	1960	30.0	Prestressed, precast, double T-girder
10	1978	42.5	Prestressed, precast, double T-girder
11	1950	36.5	Prestressed, precast, channel girder
12	1962	20.3	Prestressed, precast, double T-girder
13	1962	27.5	Prestressed, precast, double T-girder
14	1940	27.5	Prestressed, precast, double T-girder
15	1940	26.7	Prestressed, precast, double T- and concrete slab
16	1965	49.8	Prestressed, precast, double T-girder

2. PROJECT PURPOSE AND OBJECTIVE

County bridge inspectors visually rated each of the 16 bridges. The purpose of this project is to determine the bridges' load ratings based on a comprehensive structural analyses and then compare them to the visual ratings. Since no plans or specifications were available for the bridges, it was not possible to determine the exact rating from the analysis. Instead, a systematic approach was taken to determine the parameters necessary to provide the load-carrying capacity required by current code.

3. TECHNICAL APPROACH

The approach in this study consists of three major tasks:

- Site inspection
- Material testing
- Structural analysis

3.1 Site Inspection

Mr. Ron Winne, the Larimer County engineer, provided inspection reports for all of the bridges. The inspection reports contain bridge history information, plan and elevation drawings, and details of asphalt and concrete overlay thicknesses, but geometric details of the girder cross-sections are not provided. Site visits were conducted to measure the dimensions of girders on all the bridges. Drawings of girder cross-sections for all bridges can be found in Appendix A.

3.2 Material Properties

The concrete and steel properties were unknown because no specifications were available regarding the bridges. While inspecting Bridge 12, several pieces of concrete were discovered on the creek bed and in the water, as shown in Figure 3.1. One of the pieces was retrieved as a sample to perform lab testing. The concrete was cut into 2” x 2” x 2” cubes with a diamond saw, as shown in Figure 3.2. Three specimens were cut from the concrete piece and tested to determine the compressive strength of concrete. The concrete specimens and the test setup are shown in photos in Figures 3.3 and 3.4, respectively. The samples were loaded at a rate of 10,000 lbs/minute. According to the article by David J. Elwell, *Compression Testing of Concrete: Cylinders vs. Cubes*, past research indicates “cylinder/cube strength ratio to be between 0.65 and 0.90.” In this case, the compressive strength (f'_c from cylinder test) of concrete is taken as 80% of the values obtained from the 2” cube tests. The results are listed in Table 3.1.

Table 3.1 Concrete Sample Strength

Specimen	Breaking Force (lbs)	Stress (ksi)	Equivalent f'_c (ksi)
1	24000	6	4.8
2	34400	8.6	6.88
3	16800	4.2	3.36
		Avg.	5.01

Since there are was a limited number of samples from the damaged concrete layer, and the variance is too large to be conclusive, the results are not used in the analysis. The variance may be due to the imperfect cutting of the cubes. If the sides of the cube are not perfectly parallel, one corner of the cube is loaded before the compression plates come into contact with the rest of the surface. This corner of the cube will start to fail and crack, causing the sample to fail at a stress lower than the actual strength. If more samples are tested, a more reliable f'_c can be found. In addition, as seen in Figure 3.3, the aggregate size is large relative to the specimen size, which may contribute to variations as well.

Figure 3.1 Concrete pieces from streambed underneath Bridge 12.

Figure 3.2 Cutting the 2” cubes.

Figure 3.3 Three concrete cubes for testing.

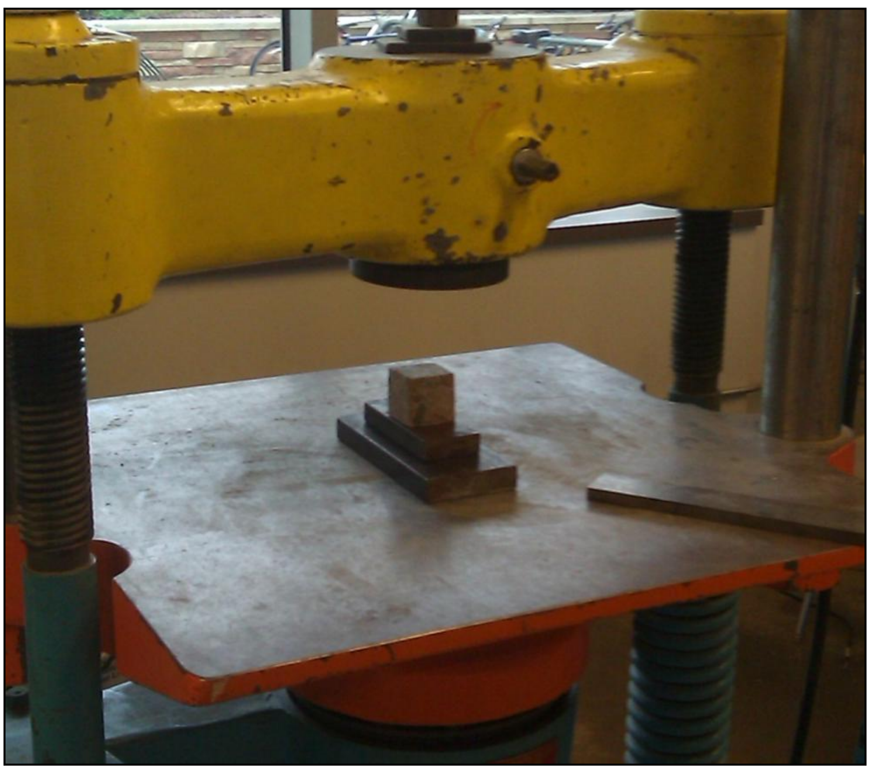

Figure 3.4 Compression test of the 2"x 2" concrete cube.

3.3 Structural Analysis

In the study, bridges are analyzed under both dead load and standard truck loading. Dead load includes self-weight and any other superimposed dead load on the bridge. Dynamic analysis includes application of influence lines to determine maximum moment due to truck loads. Since there are two types of bridges involved in the analysis, reinforced and prestressed concrete, different analysis approaches are taken for these bridge types.

Distribution factors for the live loads of prestressed bridges is first determined. The distribution factor indicates the fraction of the total live load moment on the bridge that each girder must carry. Due to unavailability of the plans and specifications regarding the prestressing forces and the tendon layout, it is not possible to carry out a comprehensive structural analysis. Therefore, Magnel diagrams are plotted for each bridge. The Magnel diagram, developed by Gustav Magnel, illustrates the limits of prestressed concrete strength. An area of acceptable prestressing force and tendon layout that will support the applied loading on each bridge girder is displayed by its Magnel diagram.

Since no plans are available regarding the reinforcement of the reinforced concrete bridges, the slabs are analyzed to determine minimum area of reinforcing steel that will carry the required loads.

3.3.1 Cross Section Geometry

The cross-section geometries measured during the site inspection provide the necessary parameters for the analysis. The reinforcement and prestress information are not available. The geometry of the cross section is listed in Appendix A.

3.3.2 Material Properties

Although the results from the concrete compressive tests are informative, they are deemed not sufficiently reliable to be used in the analysis. Due to the variability in the results of concrete test and unavailability of the specifications regarding steel, common values indicated in the AASHTO's Manual for Bridge Evaluation are used in the analysis.

CONCRETE

According to the *Manual for Bridge Evaluation*, Table 6A.5.2.1-1, concrete with unknown compressive strength in bridges built in 1959 or later is assumed to have a compressive strength, f'_c of 3.0 ksi; concrete in bridges built prior to 1959 is assumed to have an f'_c of 2.5 ksi. The f'_c for prestressed concrete is assumed to be 1.25 times larger than that of reinforced concrete. The concrete strength at transfer f'_{ci} can be taken as $0.8(f'_c)$ (Nawy 2010).

REINFORCING AND PRESTRESSING STEEL

According to the *Manual for Bridge Evaluation*, Table 6A.5.2.2-1, the yielding strength f_y of reinforcing steel for bridges built before 1954 can be assumed to be 33 ksi. The ultimate strength of the prestressing strands, f_{pu}, can be taken as 232 ksi for bridges built before 1963 and 250 ksi for bridges built in 1963 or later.

3.3.3 Loads

A variety of loading conditions were considered in this study to evaluate the sufficiency of the bridges. These loading conditions were listed in detail below.

DEAD LOAD MOMENTS

The dead load on the structure is computed using unit weights of bridge materials and the geometries measured during the site inspection. Since precise data is not available regarding the unit weight of the material, common unit weights are used in the computation. The asphalt and concrete unit weights used in the calculations are 149.3 pcf and 150 pcf, respectively.

LIVE LOAD MOMENTS

The girders are analyzed under different loading scenarios. Each of these scenarios include different live loads, which are as follows:

- Current Design Load
  HL-93 Design Load is used per LRFD design specification. This load included a 36-ton truck and a 640 lb/ft lane load/10 foot width of lane. The load configuration is shown in Appendix B.

- HS-20 Design Load
  If a bridge fails the HL-93 loading, it is analyzed under the 36-ton truck designated as HS-20. The load configuration for the HS-20 truck is shown in Appendix B. It should be noted that this loading case does not include any type of lane load. This analysis indicates whether the bridge would have met code requirements before lane loads were added to the design codes.

- Type 3 Unit Load with Lane Load
  If a bridge fails the HS-20 loading, it is analyzed under 25-ton loading in accordance with AASHTO Bridge Evaluation Manual article 6A.4.4.2.1.a. The load configuration for this load designated as Type 3 Unit is shown in Appendix B.

- Type 3 Unit Load without Lane Load
  If a bridge fails the Type 3 Unit Load with Lane Load, it is analyzed without the lane load.

DYNAMIC LOAD ALLOWANCE

A 33% impact factor is included in this study for live loads.

3.3.4 Distribution Factors for Prestressed Bridges

While the exterior girder moment may be controlling in some cases, the first interior girder moment is assumed to be controlling in this analysis. The calculation for the exterior girder moment includes the one design lane lever rule analysis and diaphragm analysis, which are beyond the scope of this project. The bridge types are defined in AASHTO LRFD Table 4.6.2.2.1-1 and the distribution factor (DF) equations are given in Table 4.6.2.2.2b-1.

AASHTO BRIDGE TYPES e, i, AND j

This category of bridge girders includes T- and double T- girders and cast-in-place monolithic concrete T-beams. The following equations are used to determine the distribution factors.

One lane loaded:

$$DF = 0.06 + \left(\frac{S}{4300}\right)^{0.4}\left(\frac{S}{L}\right)^{0.3}\left(\frac{K_g}{Lt_s}\right)^{0.1} \qquad \text{(eq. 1)}$$

Two or more lanes loaded:

$$DF = 0.075 + \left(\frac{S}{2900}\right)^{0.6}\left(\frac{S}{L}\right)^{0.2}\left(\frac{K_g}{Lt_s}\right)^{0.1} \qquad \text{(eq. 2)}$$

where:

- L(Length)-The span of the bridge. This value is taken from the county inspection reports (mm).
- S(spacing)-The width of the bridge divided by the number of girders (mm).
- I= moment of inertia of the beam (mm^4)*.
- A=cross-sectional area of the beam (mm)*.
- ts = depth of concrete slab (mm).
- K_G-Longitudinal stiffness parameter (mm^4).

* I and A are calculated for the non-composite cross-sections.

$$K_G = n(I + Ae_g^2) \qquad \text{(eq. 3)}$$

where:

$$n = \frac{E_B}{E_D} \qquad \text{(eq. 4)}$$

E_B = modulus of elasticity of beam material (MPa)
E_D = modulus of elasticity of beam deck (MPa)

Since the concrete properties were unknown, n was assumed to be 1, which was a conservative assumption for all cases. The limitations on the variables used in equations 1 and 2 were:

- $1100 \leq S \leq 4900$
- $110 \leq ts \leq 300$
- $6000 \leq L \leq 73000$
- $N_b \geq 4$ (the bridge must be comprised of at least four girders)
- $4x10^9 \leq K_g \leq 3x10^{12}$

The DF used in the analysis is the greater of the DFs calculated using eq. 1 and eq. 2. In the case that the bridge is comprised of three girders, $N_b = 3$, the DF used is the lesser of the DF found using the above equations and the DF found using the lever rule.

The Lever Rule:

$$DF_L = DF_{1\ or\ 2} * e \qquad \text{(eq. 1)}$$

Where:

$$e = 0.77 * \frac{d_e}{2800}$$

d_e=distance from the centerline of the exterior girder to the inside face of the curb (mm).
$DF_{1\text{ or }2}$ = the greater of equations 1 and 2.

It should be noted that only bridges 1 and 14 are comprised of three girders.

AASHTO BRIDGE TYPE g

AASHTO Bridge Type g is composed of pre-cast prestressed box girders. Bridge 3 is the only bridge of this type in this analysis.

One lane loaded:

$$DF = k\left(\frac{b}{2.8L}\right)^{0.5}\left(\frac{I}{J}\right)^{0.25} \qquad \text{(eq. 6)}$$

Where:

$$k = 2.5(N_b)^{-0.2} \geq 1.5 \qquad \text{(eq. 7)}$$

b = width of beam (mm)
N_b = the number of beams
I = moment of inertia (mm^4)

and:

$$J = \frac{4A_o^2}{\Sigma \frac{s}{t}} \quad \text{(eq. 8)}$$

Where:

b = width of beam (mm)
t = thickness of plate (mm)
A = Area of cross-section (mm^2)
I_p = polar moment of inertia (mm^4)
A_o = Area enclosed by centerlines of elements (mm^2)
s = length of side element

Two or more lanes loaded:

$$DF = k\left(\frac{b}{7600}\right)^{0.6}\left(\frac{b}{L}\right)^{0.2}\left(\frac{I}{J}\right)^{0.06} \quad \text{(eq. 9)}$$

The design DF is the larger of equations 6 and 9.
The limitations on equations 6 and 9 are as follows:

- $900 \leq b \leq 1500$
- $6000 \leq L \leq 37000$
- $5 \leq N_b \leq 20$

AASHTO BRIDGE TYPE h

AASHTO Type h is a U-channel, pre-cast, prestressed girder. Bridge 11 is comprised of type h girders. The distribution factor for type h can be found using eq. 10 and can only be true if the following applies:

Skew $\leq$ 45°
$N_L(number\ of\ lanes) \leq 6$

Equation 10 can be used regardless of the number of loaded lanes.

$$DF = S/D \quad \text{(eq. 10)}$$

Where:

$$C = K\left(\frac{W}{L}\right) \leq K \quad \text{(eq. 2)}$$

$$D = 300[11.5 - N_L + 1.4N_L(1 - 0.2C)^2] \quad \text{(eq. 12)}$$

When C$\leq$5

$$D = 300(11.5 - N_L) \quad \text{(eq. 13)}$$

When C>5

K =2.2 For preliminary design
S = Spacing of beams or webs (mm)
W = edge-to-edge width of bridge (mm)
L = span of bridge (mm)

3.3.5 Composite Action

Bridges 1, 4, 8, and 10 are overlaid with a concrete slab. This causes composite action during loading of the bridge. To be conservative, composite action is not considered in the analysis.

3.3.6 Magnel Diagrams for Prestressed Bridges

The Magnel Diagram is a useful tool to determine the relationship between the eccentricity of the strands, e, and the prestressing force, P, based on the given girder cross-section and material properties. The equations plotted for the Magnel diagram are shown below. These equations are based on transfer and serviceability conditions. Equations 1 and 2 ensure that the stress due to the self-weight of the girder does not exceed the tension limit at the top and the compression limit at the bottom of the girder, respectively. Equations 3 and 4 ensure that the stress due to the total service loads does not exceed the compression limit at the top and the tension limit at the bottom of the girder respectively. Sample calculations for the Magnel Diagram of Bridge 1 are shown in Appendix C.

$$\frac{1}{P_i} \geq \frac{{}^{e}/_{k_b} - 1}{\left(\frac{M_g C_t}{I_g} + 3\sqrt{f'_{ci}}\right) A_g} \cdots\cdots\cdots\cdots Equation\ 1 \quad \text{(eq. 3)}$$

$$\frac{1}{P_i} \geq \frac{{}^{e}/_{k_t} + 1}{\left(\frac{M_g C_b}{I_g} + 0.6 f'_{ci}\right) A_g} \cdots\cdots\cdots\cdots Equation\ 2 \quad \text{(eq. 4)}$$

$$\frac{1}{P_i} \leq \frac{\left({}^{e}/_{k_b} - 1\right)\eta}{\left(\frac{M_T C_t}{I_g} - 0.45 f'_{c}\right) A_g} \cdots\cdots\cdots\cdots Equation\ 3 \quad \text{(eq. 5)}$$

$$\frac{1}{P_i} \leq \frac{\left({}^{e}/_{k_t} + 1\right)\eta}{\left(\frac{M_T C_b}{I_g} - 6\sqrt{f'_{c}}\right) A_g} \cdots\cdots\cdots\cdots Equation\ 4 \quad \text{(eq. 6)}$$

Where:

$P_i = Prestress\ at\ transfer$
$e = Eccentricity\ of\ the\ strands$
$A_g = Cross\ sectional\ area$

$k_b = Bottom\ kern\ point$
$k_t = Top\ kern\ point$
$C_t = Distance\ from\ centroid\ to\ top\ fiber$
$C_b = Distance\ from\ centroid\ to\ bottom\ fiber$
$I_g = Moment\ of\ inertia\ of\ the\ cross\ sectional\ area$
$M_g = Moment\ due\ to\ self - weight\ of\ the\ girder$
$M_T = Total\ moment\ due\ to\ service\ loads$
$\eta = Prestressing\ factor$
$f'_{ci} = Compressive\ strength\ of\ concrete\ at\ transfer\ (0.8f'_c)$
$f'_c = Compressive\ strength\ of\ concrete\ at\ the\ end\ of\ 28\ days$

According to the *Manual for Bridge Evaluation*, the ultimate strength of the prestressing strands, f_{pu}, can be taken as 232 ksi for bridges built before 1963 and 250 ksi for bridges built in 1963 or later. Conservatively assuming 232 ksi as f_{pu}, the prestress immediately after transfer (f_{pi}) is $0.74f_{pu}$ (Nawy, 2010).

$$f_{pi} = 0.74 \times f_{pu} \quad \text{(eq. 17)}$$

$$f_{pi} = 0.74 \times 232 = 171.68 \quad \text{(eq. 8)}$$

Where:

f_{pi} = Stress in prestressing tendon immediately after transfer (ksi)
f_{pu} = Ultimate stress for prestressing tendon (232 ksi)

From ACI Code Commentary (1963, 1971, 1977), the lump sum losses of 35 ksi for prestressing that appeared in the 1963 report of Committee 423 generally give satisfactory results for many applications.

$$f_{pi} - 35 = f_{pe} \quad \text{(eq. 19)}$$

$$171.68\ ksi - 35\ ksi = 136.68\ ksi$$

Where:

f_{pi} = Stress in prestressing tendon immediately after transfer (171.68 ksi)
f_{pe} = Effective stress in the prestressing tendon after losses (ksi)

$$\frac{f_{pe}}{f_{pi}} = \frac{p_e}{p_i} = \eta \quad \text{(eq. 20)}$$

$$\frac{136.68\ ksi}{171.68\ ksi} = 0.79613$$

Where:

f_{pe} = Effective stress in the prestressing tendon after losses (136.68 ksi)
f_{pi} = Stress in prestressing tendon immediately after transfer (171.68 ksi)
p_e = Effective force in prestressing tendon (kips)
p_i = Initial force in prestressing tendon (kips)
η = Prestressing factor

Therefore, it is felt that a reasonable prestressing factor is 0.80 or 80%.

After plotting the above equations, different combinations of prestressing force, P, and eccentricity, e, can be obtained from the area that satisfies the equations. The Magnel diagrams generated for the prestressed bridges are shown in Appendix D. The shaded areas in between the lines are the different combinations of force and prestress that can satisfy all the equations.

3.3.7 Reinforced Slab Bridges

The moments used in the analysis for the reinforced bridges are found in the same manner as the moments for the prestressed bridges. The live load moment is not reduced by a distribution factor because there are no load distributions involved in the system; the slab carries the total moment. The minimum areas of reinforcement needed to carry the required loads are calculated for different loading scenarios.

4. RESULTS

Table 4.1 shows the distribution factors calculated for each bridge and the DFs used in the analysis.

Table 4.1 Interior Beam Distribution Factors

Bridge #	Girder Type	DF One-Lane	DF Multi-Lane	DF Lever Rule	DF Design
1	j	0.458	0.636	0.722	0.635
2	i	0.418	0.511	N/A	0.511
3	g	0.124	0.214	N/A	0.214
4	i	0.384	0.508	N/A	0.508
5	i	0.444	0.530	N/A	0.530
6	i	0.479	0.622	N/A	0.622
7	N/A	N/A	N/A	N/A	N/A
8	I	0.389	0.531	N/A	0.531
9	e	0.495	0.629	N/A	0.629
10	i	0.451	0.588	N/A	0.588
11	h	0.283		N/A	0.284
12	i	0.436	0.521	N/A	0.521
13	i	0.416	0.510	N/A	0.510
14	i	0.516	0.651	0.731	0.651
15	N/A	N/A	N/A	N/A	N/A
16	i	0.413	0.541	N/A	0.541

As previously mentioned, the bridges are analyzed under different loading scenarios. The Magnel diagrams are constructed to determine combinations of prestressing force and eccentricity that would carry the required loads. The Magnel diagrams for the bridges are given in Appendix D.

The existence of the combinations of prestressing force and eccentricity specifies a viable solution to the prestressing equations and thus indicates that the bridge would pass under the given loading scenario. In other words, the existence of the shaded area indicates that the bridge could pass the loading requirement, i.e., there is a possible combination, but it is not certain (due to the lack of information for the prestressing tendon configuration) that the possible combination is the actual combination for the given bridge girder. Table 4.2 summarizes the results for different loadings scenarios.

Table 4.2 Bridge Analysis Results

Bridge #	Loading scenarios			
	HL-93 36 Ton Truck	HS-20, 36 ton truck, no lane load	Type 3 25 Ton Truck with lane load	Type 3 25 Ton Truck with no lane load
1	Fail	Fail	Fail	Fail
2	Fail	Fail	Fail	Fail
3	Fail	Fail	Fail	Pass
4	Fail	Fail	Fail	Fail
5	Fail	Pass	Pass	Pass
6	Fail	Fail	Fail	Fail
7	Not analyzed	Not analyzed	Not analyzed	Not analyzed
8	Fail	Fail	Fail	Fail
9	Pass	Pass	Pass	Pass
10	Fail	Fail	Fail	Fail
11	Fail	Fail	Fail	Pass
12	Pass	Pass	Pass	Pass
13	Pass	Pass	Pass	Pass
14	Fail	Fail	Fail	Fail
15	Not analyzed	Not analyzed	Not analyzed	Not analyzed
16	Fail	Fail	Fail	Pass

The maximum moment reductions required to allow the bridges that fail all load cases to pass the Type 3 load without lane loading are shown in Appendix D.

Bridge 7 was analyzed as a reinforced slab. The calculation of the minimum reinforcement that would carry the specified loads is shown in Appendix C, and the minimum reinforcement area is shown in Table 4.3.

Table 4.3 Required Area of Reinforcement for Bridge 7

Bridge 7	Loading scenarios			
	HL-93 36-Ton Truck	HS-20, 36-ton truck, no lane load	Type 3 25-Ton Truck with lane load	Type 3 25-Ton Truck with no lane load
Area of Reinforcement (in^2/ft)	2.8	2.6	2.6	2.4

Bridge 15 is not analyzed because it was constructed with a combination of a reinforced slab and prestressed girders. The hybrid nature of the construction, coupled with the lack of drawings or specifications, results in the analysis for Bridge 15 being beyond the scope of this project.

5. DISCUSSION

The bridges that are deficient in flexural strength for the design loadings in the structural analysis have no possible combinations of eccentricity and prestressing force that could support the loads. An objective of the analysis is to establish whether or not the load carrying capacities of the bridges could even satisfy current code based on their geometry. It was assumed that all the bridges would pass the HS-20 load, because they are designed for that load and have all carried that load in the field for the last few decades. In this analysis, 7 of the 14 prestressed bridges fail all of the load cases, indicating that half the bridges on the list would not satisfy current design standards under the load of a 25-ton truck. The following variables and conservative assumptions may have contributed to a significant reduction in the computed load carrying capacities.

- Prestressing Force and Tendon Layout (eccentricity)

Since the prestressing forces and tendon layout are unknown, Magnel diagrams are developed from the geometry of the girders and the bridge loads. The diagrams display the possible combinations of prestressing force and tendon layout that would satisfy the load-carrying capacity required by code. The possible layouts are limited by the maximum eccentricity within each beam at midspan; maximum eccentricity is the distance from the centroid of the girder to the centroid of the prestressing tendons, which is assumed to be three inches above the bottom of the girder due to minimum coverage requirements.

Design constraints on the prestressing force are not identified in the development of the Magnel diagrams. If an upper bound on prestressing force commonly used in the 1960's could be identified, the area of possible combinations on the Magnel diagram may be reduced. The smaller area on the Magnel diagram would be more restrictive or less permissable of acceptable combinations of eccentricity and prestressing force. More information available to include in the analysis would yield a more representative area.

- Diaphragm Effects

In the AASHTO equations for interior beam distribution factors, the effect of the diaphragms is not accounted for. If the diaphragms had been considered in the structural analysis, the bridges with diaphragms may have had a larger load carrying capacity. If the bridges are analyzed with structural models, assuming all the variables are known, or if the bridges were load tested, the effects of the diaphragms would be included in the load carrying capacity.

- Concrete Strength

Because there was no available concrete strength data, conservative f'_c values are used in accordance with the AASHTO *Manual for Bridge Evaluation*. Lower concrete strengths provide lower flexural strengths. If core samples were taken from the bridges to find the actual concrete strength, it is likely that the results would indicate higher strengths than those used in the analysis. The higher concrete strengths would increase the capacities of the bridges, and fewer bridges would be deficient in flexural strength.

- Loss in Prestressing Force Over Time

Because the initial prestress is unknown, it is not possible to do a prestress loss analysis. The assumption used was that current prestress is 80% of initial prestress. If the relationship between current and initial prestress was different, there would be a large change in the Magnel diagrams, which could change the outcome of the analysis.

- Mild Steel Reinforcement

From site inspections, it is known that at least several prestressed bridges contain steel reinforcement. The concrete girders on some bridges had spalled and cracked, revealing the steel reinforcement. None of the details of reinforcement are known, therefore, the reinforcement could not be considered in the analysis. If reinforcement had been included in the analysis, the bridges would have had a larger load carrying capacity.

- Controlling Force in Analysis

It is assumed that flexure would be the controlling limit state in the structural analysis. Shear, deck, foundation, scouring, and wing-wall analyses are not conducted. If the controlling limit state of the bridges is flexure, then the omission of the other limit states will not affect the pass or fail rating. If a bridge has a controlling limit state other than flexure, additional analysis would be needed.

- Interior Beam Distribution Factor

Interior beam distribution factors are used in the structural analysis for the prestressed bridges. Exterior beam distribution factors are not calculated. In the case that an exterior beam distribution factor is higher than the interior beam distribution factor, the analysis completed herein would overestimate the actual flexural strength of the bridge, making the pass rate un-conservative.

- Bridge Records

Bridge 11 was constructed in 1950, and according to the records, has not been reconditioned or replaced. The inspection report from 1980 identifies the bridge as a prestressed double T bridge; whereas the plans and inspection reports from 2009 identify it as a U-Beam bridge. Site inspections confirm that the girders of this bridge are U-Beams. Although the bridge is assumed to be prestressed in the analysis, site inspections alone can not conclude whether the girders were prestressed. Since the bridge was constructed in 1950, it is doubtful that it is prestressed. The first prestressed bridge in the United States was built in 1950. Prestressing in Colorado did not become common until the 1960's, as seen by the construction dates of the other prestressed bridges in this analysis. It is possible that the records are incorrect and bridge 11 is not prestressed. A structural analysis of the bridge as a reinforced U-beam bridge would be needed if the records are incorrect.

- Composite Action

Composite action is not considered in the analysis. Bridges 1, 4, 8, and 10 have a significantly thick topping slab; therefore, composite action is highly probable for these bridges. Composite action contributes to the flexural capacity of the bridge, making the assumption of no composite action slightly conservative, but consistent with what is often done in bridge engineering design.

6. RECOMMENDATIONS

The results of this analysis are felt to be conservative because many unknowns must be accounted for using assumptions. Experimental determination of material values for these unknowns would make the analysis more reliable. Core samples of the concrete girders could provide a more representative concrete strength, which would likely result in larger load-carrying capacity. X-ray technology could be used to determine the layout of not only the prestressing tendons, but also of any mild steel reinforcement. Load testing the bridges would be costly, but it would be the most reliable method of ascertaining the capacities.

REFERENCES

AASHTO LRFD Bridge Design Specifications. Washington, D.C.: American Association of State Highway and Transportation Officials, 2009.

Elwell, David J., and Gongkang Fu. *Compression Testing of Concrete: Cylinders vs. Cubes*. Rep. no. 319. New York: Department of Transportation, 1995.

The Manual for Bridge Evaluation. 1st ed. Washington, DC: American Association of State Highway and Transportation Officials, 2008.

Nawy, Edward G. *Prestressed Concrete: A Fundamental Approach*. Fifth Update ed. Upper Saddle River: Prentice Hall, 2010.

APPENDIX A. PRESTRESSED GIRDER CROSS-SECTIONS

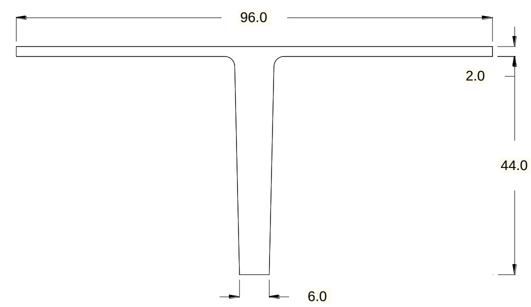

Figure A.1 Bridge 1

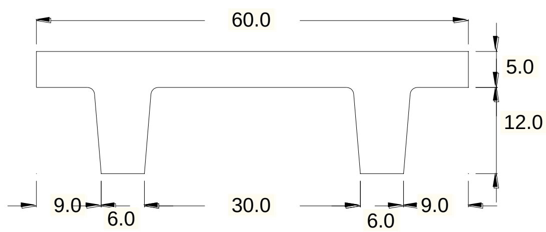

Figure A.2 Bridge 2

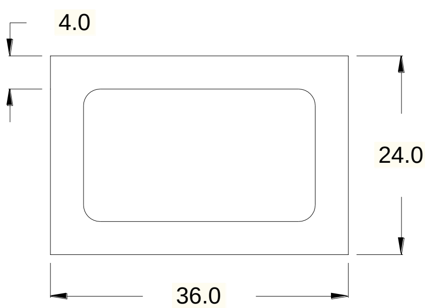

Figure A.3 Bridge 3

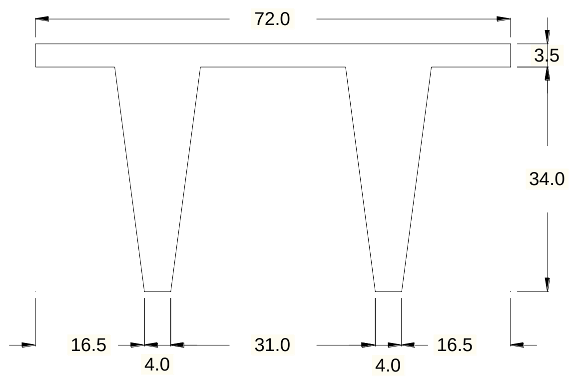

Figure A.4 Bridge 4

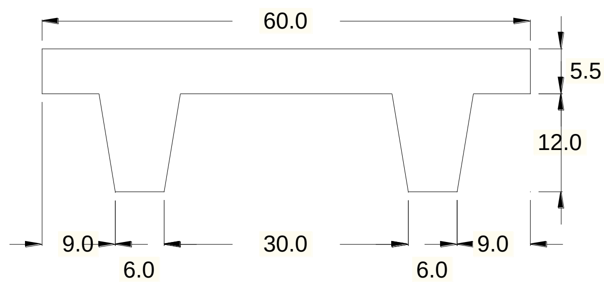

FigureA.5 Bridge 5

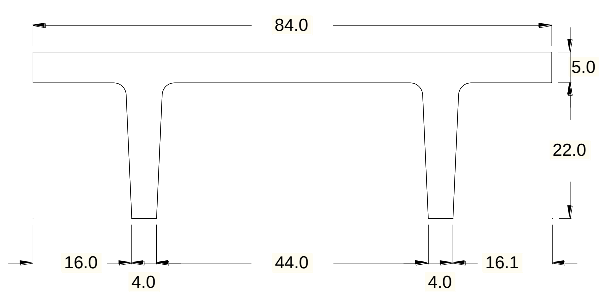

Figure A.6 Bridge 6

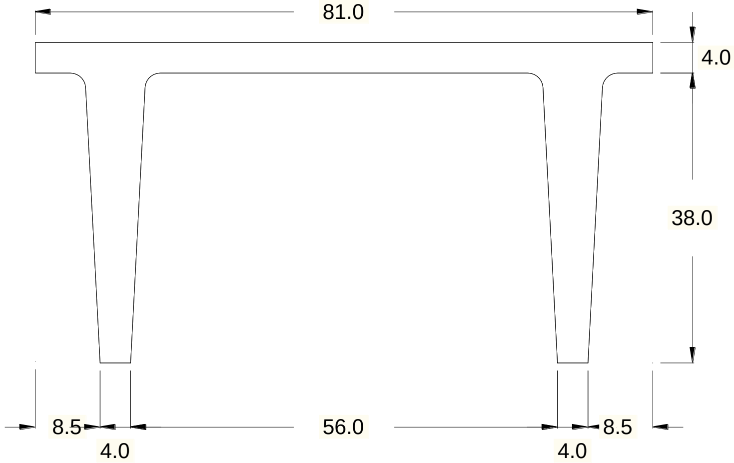

Figure A.7 Bridge 8

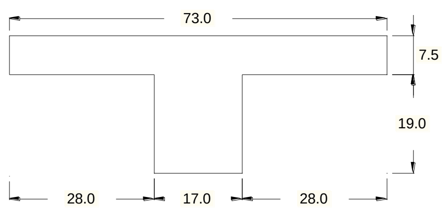

Figure A.8 Bridge 9

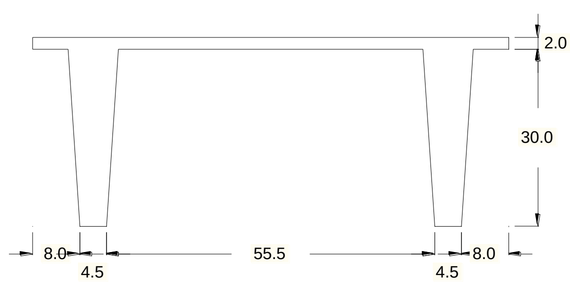

Figure A.9 Bridge 10

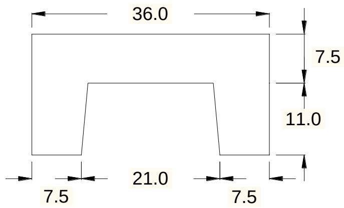

Figure A.10 Bridge 11

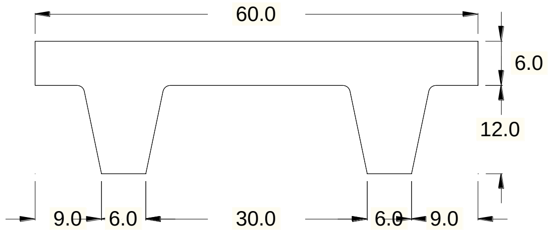

Figure A.11 Bridge 12

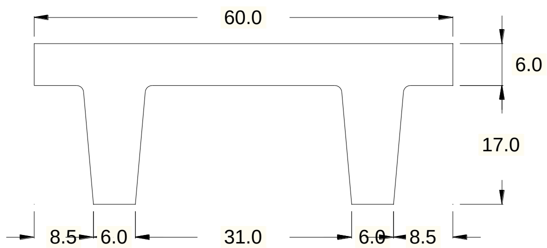

Figure A.12 Bridge 13

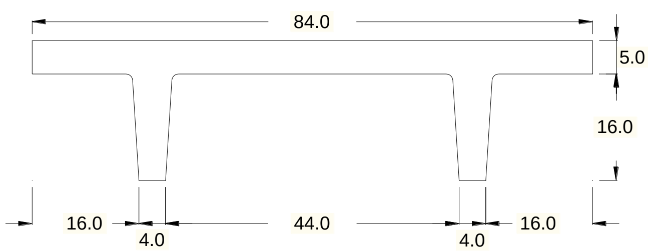

Figure A.13 Bridge 14

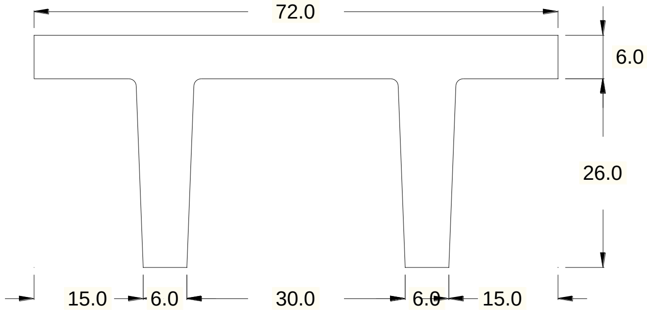

Figure A.14 Bridge 16

APPENDIX B. LOADING TRUCKS

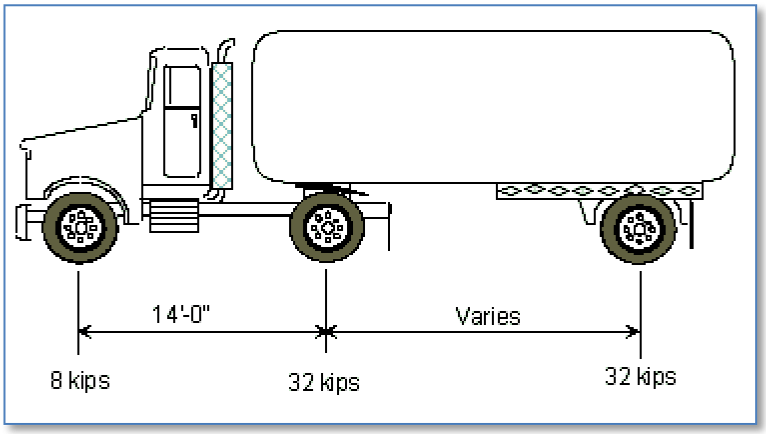

Figure B.1 HL-93 and HS-20 36 ton loading truck.

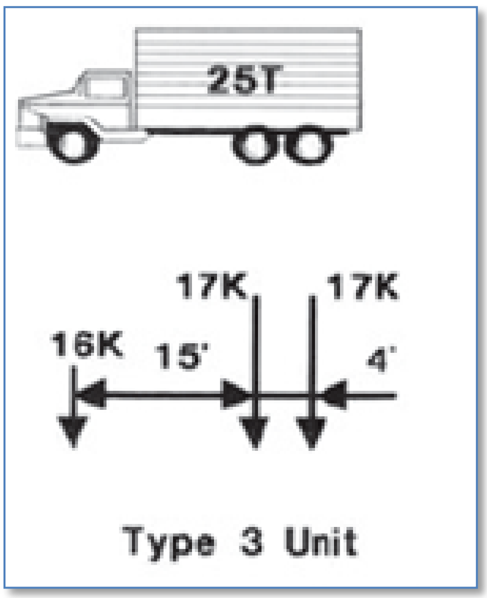

Figure B.2 HL-93 and HS-20 25 ton load truck (Type 3)

APPENDIX C. SAMPLE CALCULATIONS

Sample Calculations for Magnel Diagram – Bridge 1

$A_g = 501.64\ in^2$
$k_b = 14.66\ in$
$k_t = 6.75\ in$
$C_t = 14.5\ in$
$C_b = 31.5\ in$
$I_g = 106651.1\ in^4$
$M_g = 3758.82\ kip - in$
$M_T = 8750\ kip - in$
$\eta = 0.8$
$f'_{ci} = 3\ ksi$
$f'_c = 3.75\ ksi$

By plugging in the given values into equations 1 to 4 we get the following:

$$\frac{1}{P_i} \geq (201.345\text{e} - 295.17) * 10^{-6}\ \cdots\cdots\cdots\cdots Equation\ 1$$
$$\frac{1}{P_i} \geq (101.481\ \text{e} + 684.99) * 10^{-6} \cdots\cdots\cdots Equation\ 2$$
$$\frac{1}{P_i} \leq (-218.497e + 3203.16) * 10^{-6} \cdots\cdots\cdots\cdots Equation\ 3$$
$$\frac{1}{P_i} \leq (106.571\ \text{e} + 719.36) * 10^{-6} \cdots\cdots\cdots\cdots Equation\ 4$$

Sample Calculations for Reinforced Concrete Slab - Bridge 7

HL-93 loading with lane load

$M_g = 697.68\ kip - ft$
$M_{DS} = 188.68\ kip - ft$
$M_{LL} = 97.05 + 1.33 * 357.94\ kip - ft = 573.11\ kip - ft$

$M_u = 1.25M_{DL} + 1.7M_{LL}$
$M_u = 1.25(697.68 + 188.68\ ) + 1.75 * 573.11 = 2110.89\ kip - ft$

$$\frac{M_u}{ft} = \frac{2110.88 * 12\ kip - in}{23\ ft} = 1101.33\ kip - in/ft$$

$M_u = \emptyset M_n$
$M_n = A_S * f_y(d - \frac{a}{2})$
$\emptyset = 0.9\ for\ flexure$
$f_y = 33\ ksi$ based on AASHTO Manual for Bridge Evaluation
$d = 14.5\ in$

$\left(d - \frac{a}{2}\right) \approx 0.9d$ (Assumed)

$$A_S = \frac{M_n}{0.9d * f_y} = \frac{(1101.33\ kip - in/ft)/0.9}{0.9 * 14.5 * 33ksi} = 2.84\ in^2/ft$$

$A_S = \frac{2.84\ in^2/ft}{0.2\ in^2}$=(14 No.4)/ft

HL-93 without lane load

$M_g = 697.68\ kip - ft$
$M_{DS} = 188.68\ kip - ft$
$M_{LL} = 1.33 * 357.94\ kip - ft = 476.06\ kip - ft$

$M_u = 1.25M_{DL} + 1.7M_{LL}$
$M_u = 1.25(697.68 + 188.68\ ) + 1.75 * 476.06 = 1941.1\ kip - ft$

$$\frac{M_u}{ft} = \frac{1941.1 * 12\ kip - in}{23\ ft} = 1012.8\ kip - in/ft$$

$M_u = \emptyset M_n$
$M_n = A_S * f_y(d - \frac{a}{2})$
$\emptyset = 0.9\ for\ flexure$
$f_y = 33\ ksi$ based on AASHTO Manual for Bridge Evaluation
$d = 14.5\ in$

$\left(d - \frac{a}{2}\right) \approx 0.9d$ (Assumed)

$$A_S = \frac{M_n}{0.9d * f_y} = \frac{(1012.8\ kip - in/ft)/0.9}{0.9 * 14.5 * 33ksi} = 2.61\ in^2/ft$$

$A_S = \frac{2.61\ in^2/ft}{0.2\ in^2}$ = (13 No.4)/ft

Type 3 Unit Load

$M_g = 697.68\ kip - ft$
$M_{DS} = 188.68\ kip - ft$
$M_{LL} = 97.05 + 1.33 * 285.49\ kip - ft = 476.75\ kip - ft$

Same as previous one.

Type 3 Unit Load without lane load

$M_g = 697.68\ kip - ft$
$M_{DS} = 188.68\ kip - ft$
$M_{LL} = 1.33 * 285.49\ kip - ft = 379.7\ kip - ft$

$M_u = 1.25M_{DL} + 1.7M_{LL}$
$M_u = 1.25(697.68 + 188.68\ ) + 1.75 * 379.7 = 1772.4kip - ft$

$$\frac{M_u}{ft} = \frac{1772.4 * 12\ kip - in}{23\ ft} = 924.73\ kip - in/ft$$

$M_u = \emptyset M_n$
$M_n = A_S * f_y(d - \frac{a}{2})$
$\emptyset = 0.9\ for\ flexure$
$f_y = 33\ ksi$ based on AASHTO Manual for Bridge Evaluation
$d = 14.5\ in$

$\left(d - \frac{a}{2}\right) \approx 0.9d$ (Assumed)

$$A_S = \frac{M_n}{0.9d * f_y} = \frac{(924.73\ kip - in/ft)/0.9}{0.9 * 14.5 * 33ksi} = 2.38\ in^2/ft$$

$A_S = \frac{2.36\ in^2/ft}{0.2\ in^2}$=(12 No.4)/ft

APPENDIX D. MAGNEL DIAGRAMS

Bridge(s) passing HL-93 36-Ton Truck (pass 1)

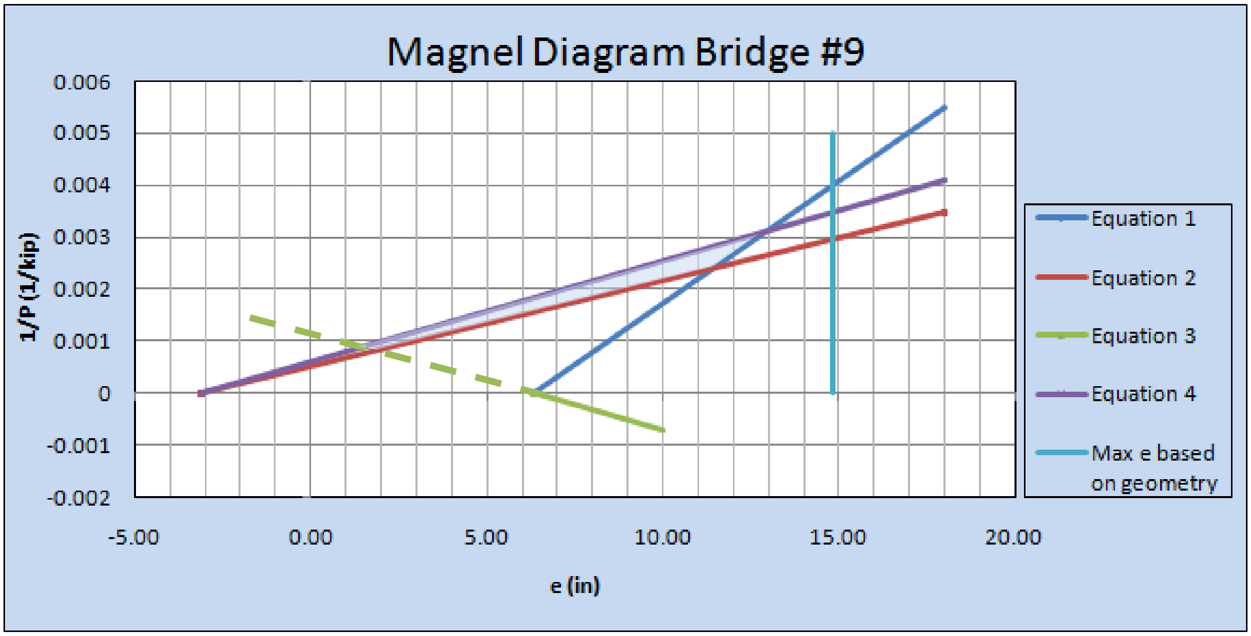

Figure D.1 Bridge 9 - Pass 1

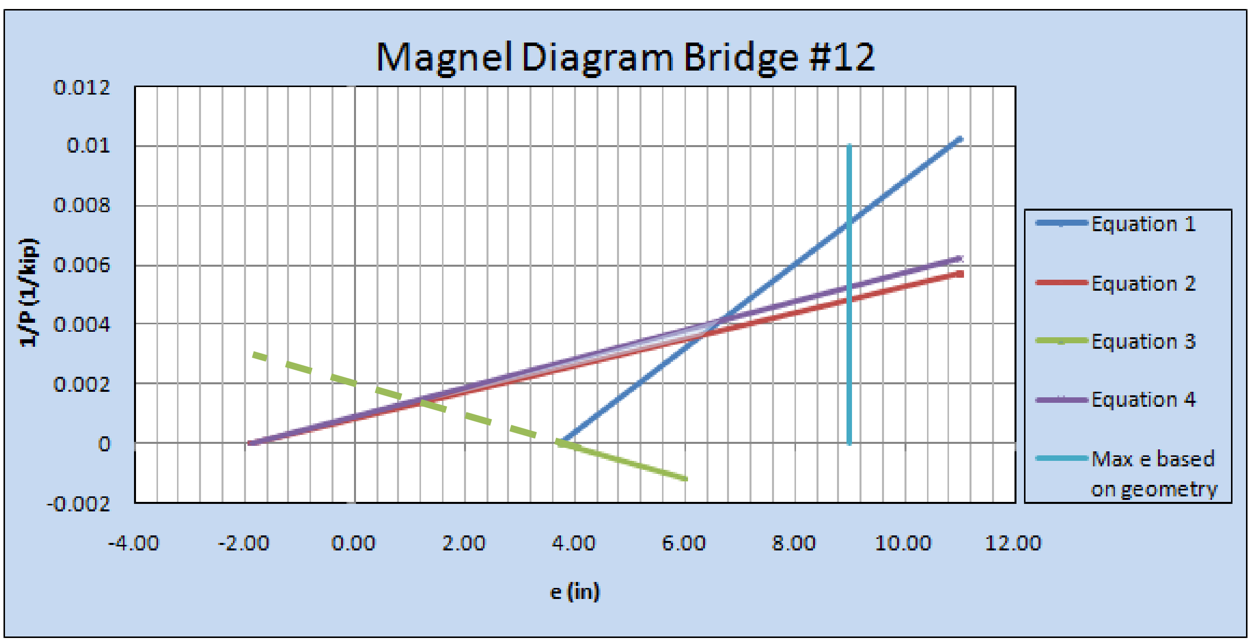

Figure D.2 Bridge 12 - Pass 1

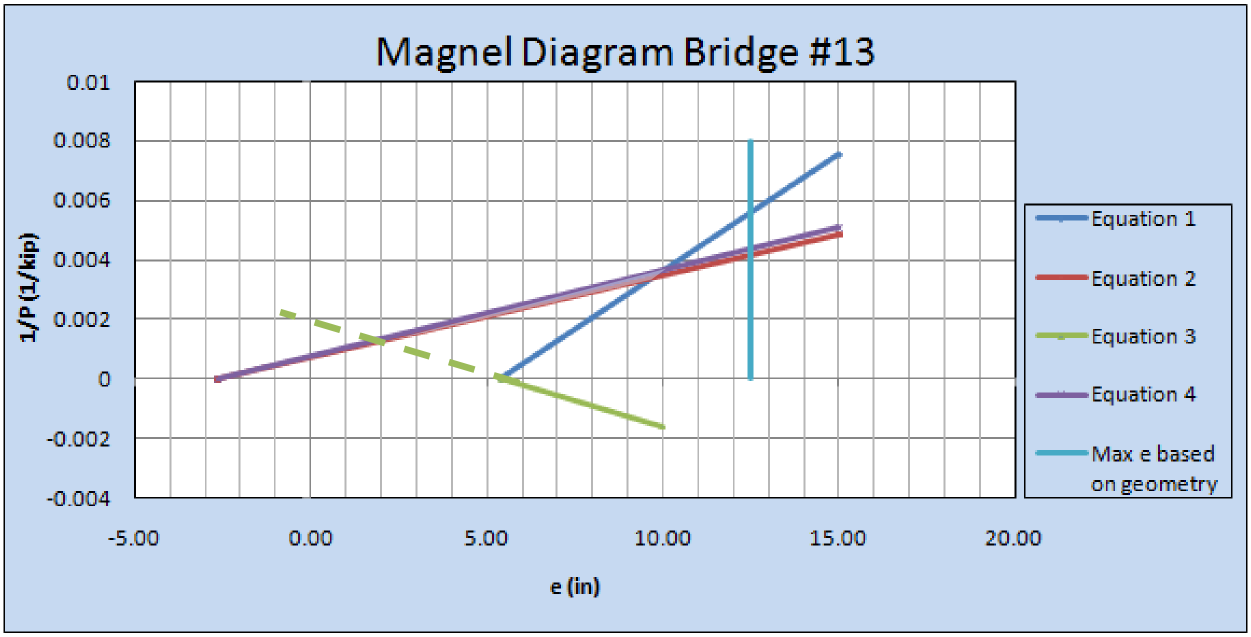

Figure D.3 Bridge 13 - Pass 1

Bridge(s) passing HS-20, 36-Ton Truck, No Lane Load (Pass 2)

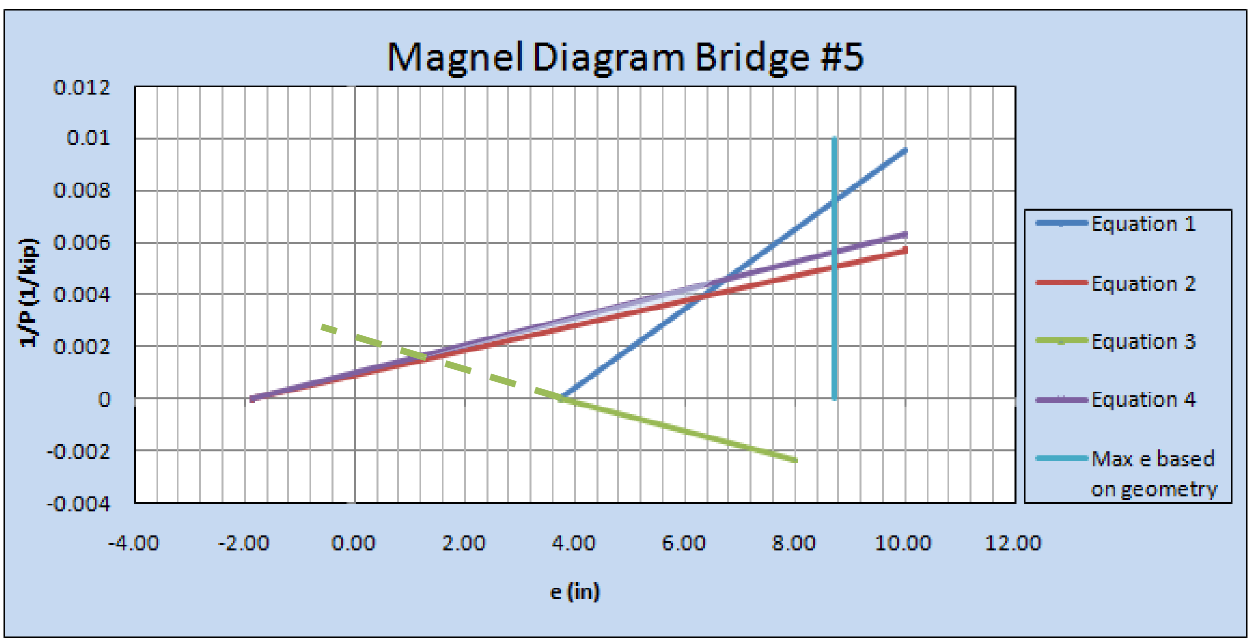

Figure D.4 Bridge 5 - Pass 2

Bridges Passing Type 3 25-Ton Truck Without Lane Load (Pass 4)

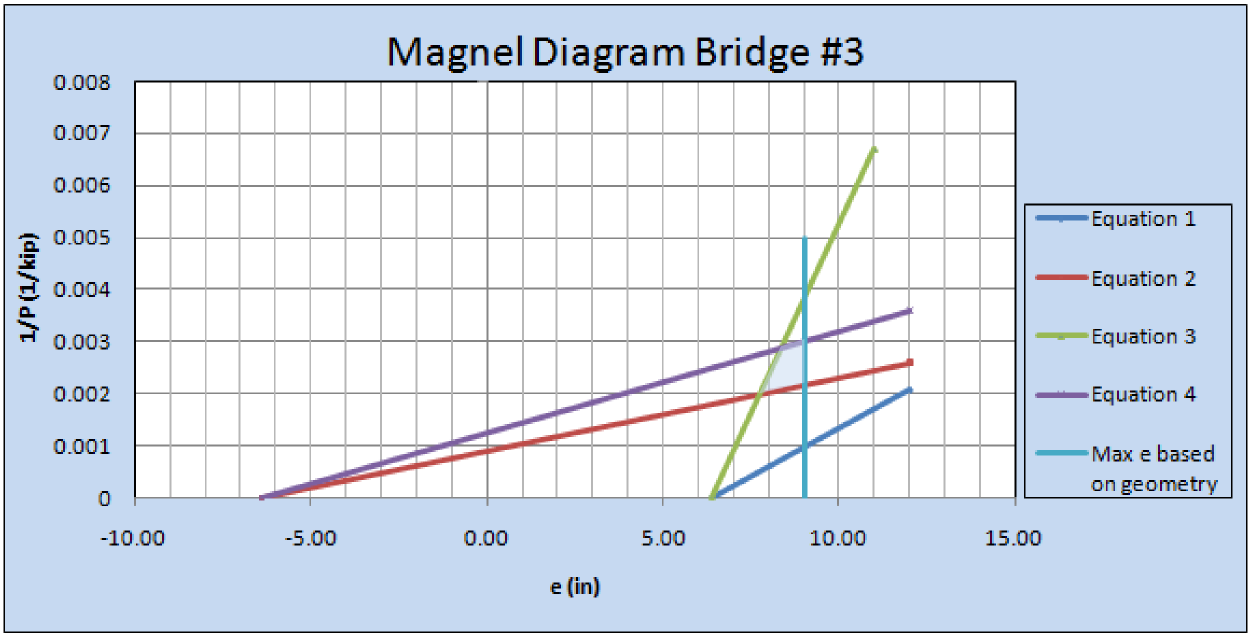

Figure D.5 Bridge 3 - Pass 4

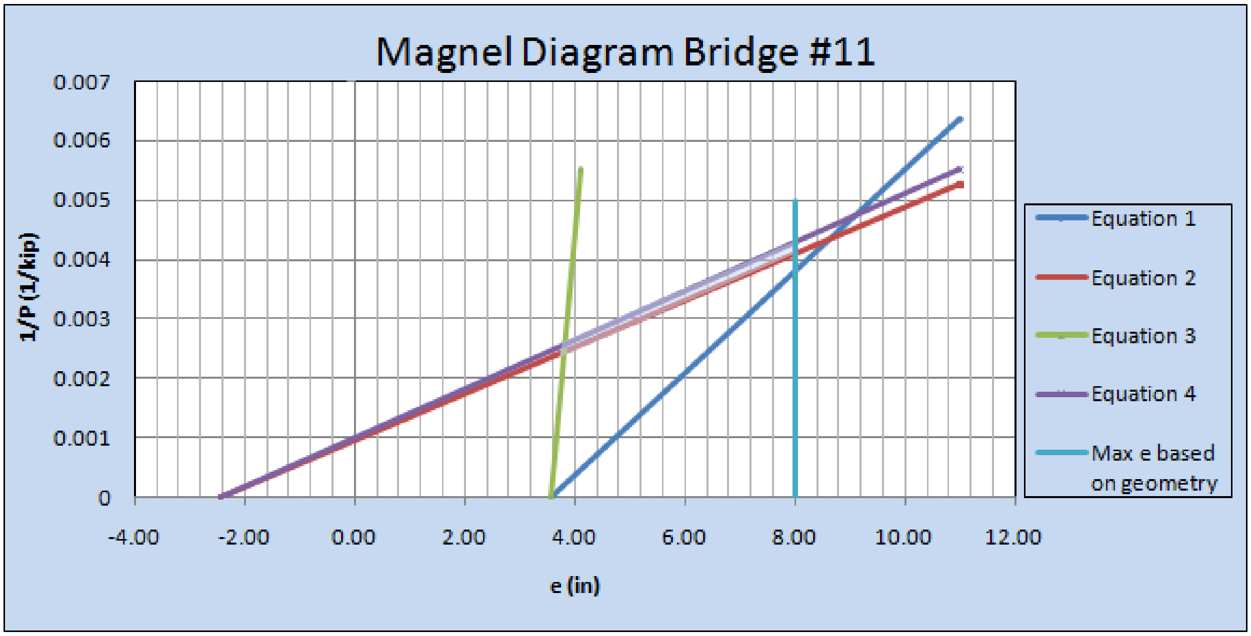

Figure D.6 Bridge 11 - Pass 4

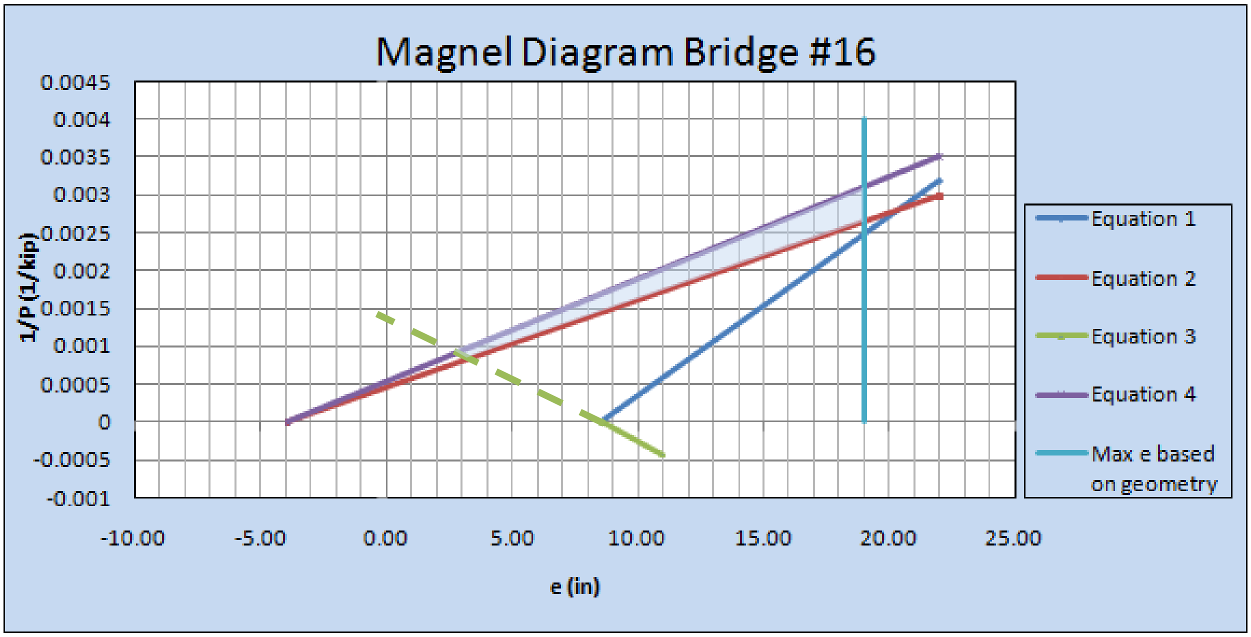

Figure D.7 Bridge 16 - Pass 4

Bridges with Maximum Moment Reduction Passing Type 3 25-Ton Truck without lane load

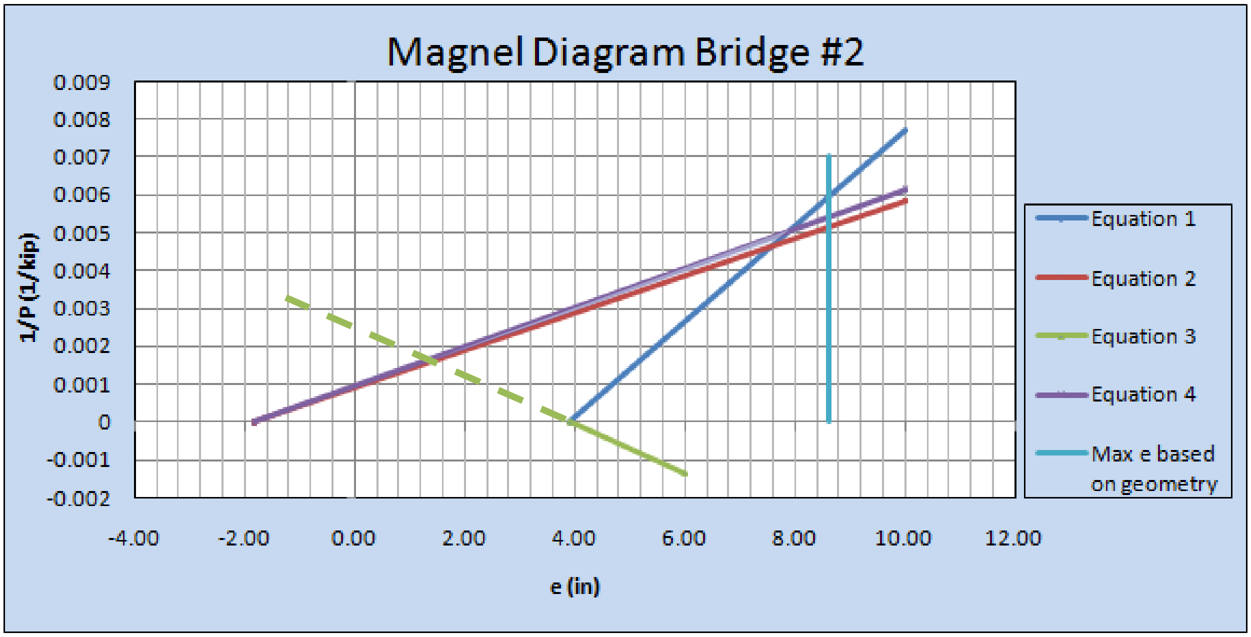

Figure D.8 (Bridge 2) 77% Max Moment (1850 kip-in)

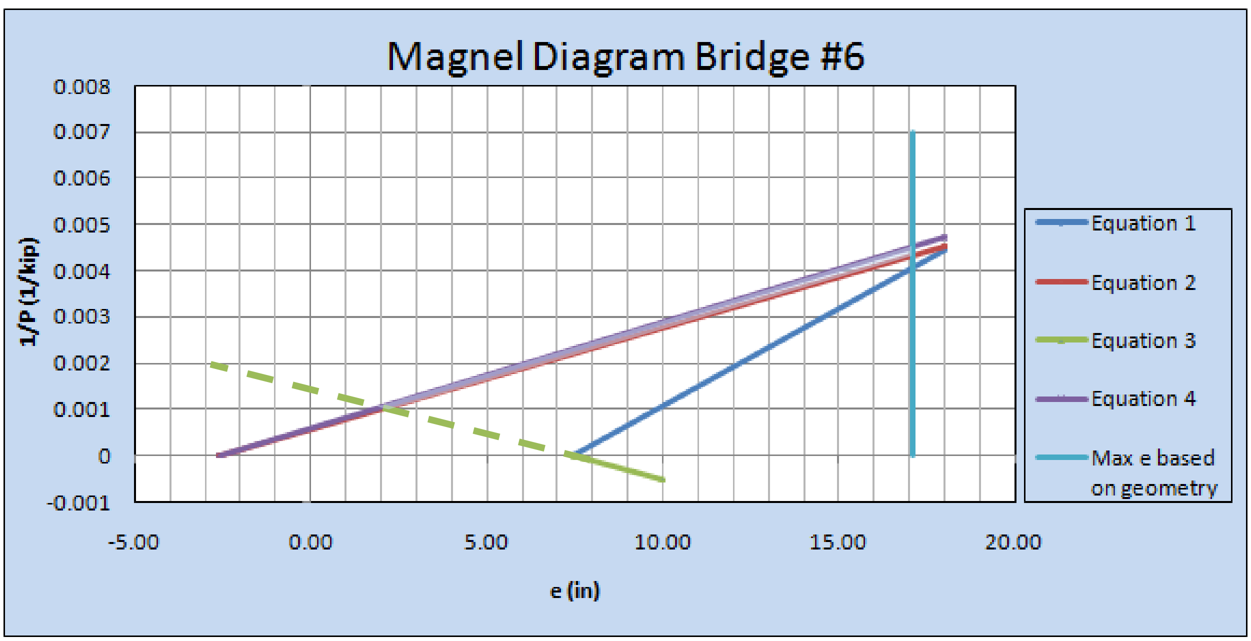

Figure D.9 (Bridge 6) 60% Max Moment (4100 kip-in)

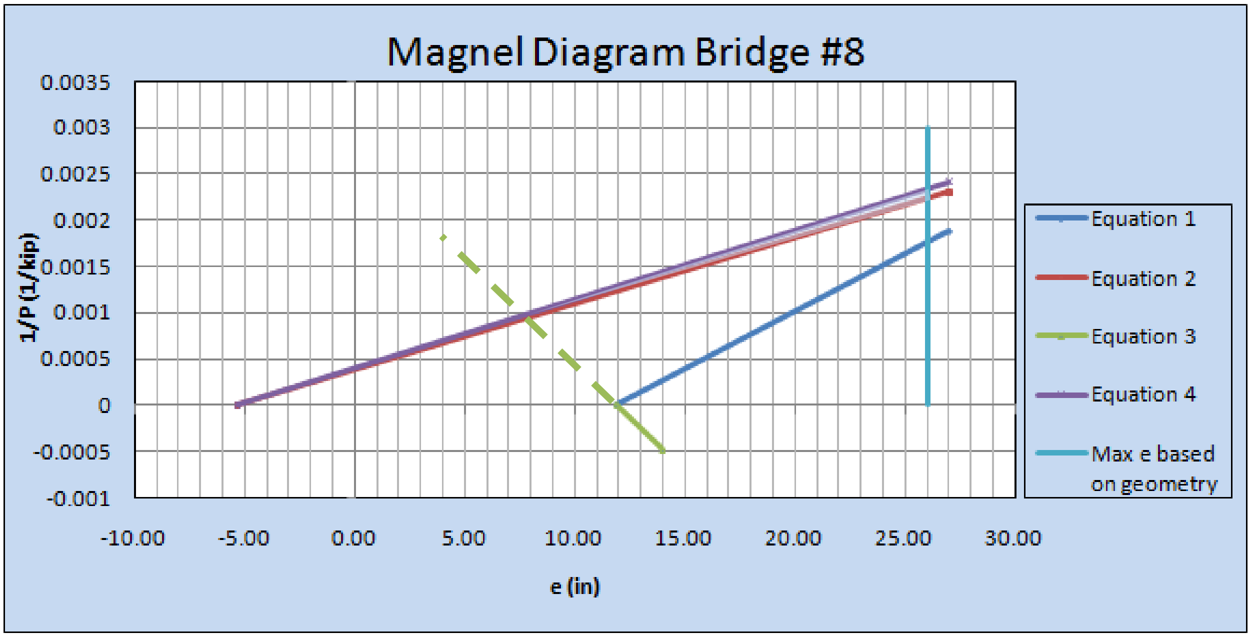

Figure D.10 (Bridge 8) 64.3% Max Moment (12250 kip-in)

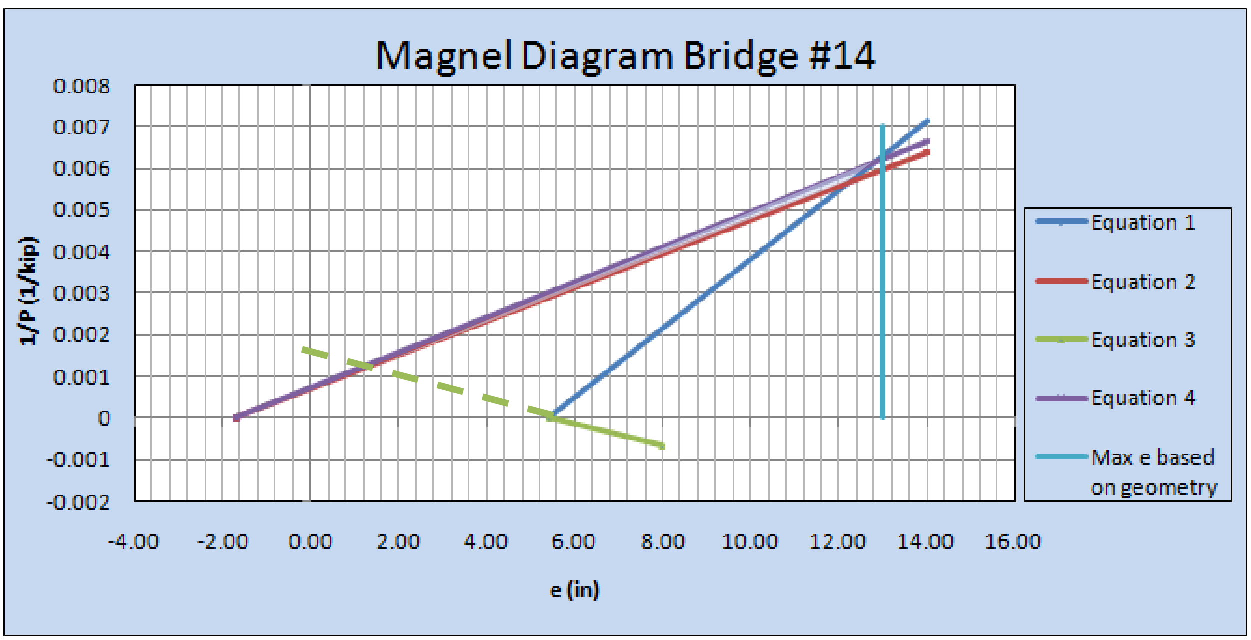

FigureD.11 (Bridge 14) 69.3% Max Moment (2250 kip-in)

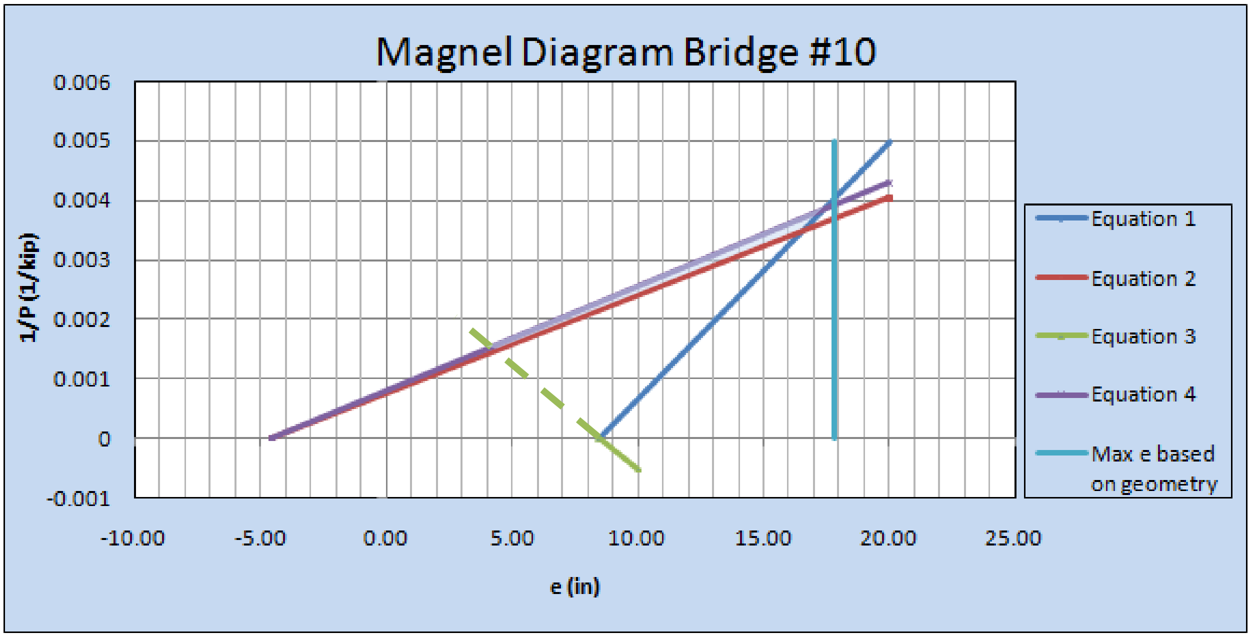

Figure D.12 (Bridge 10) 73 % Max Moment (5500 kip-in)

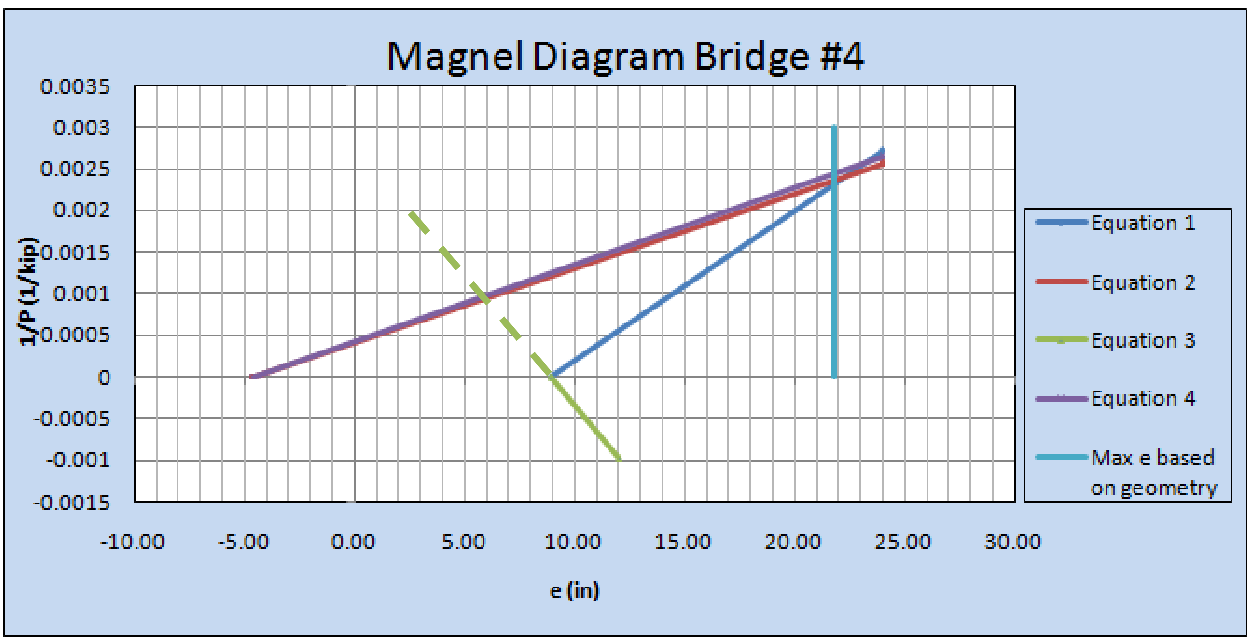

Figure D.13 (Bridge 4) 71.8% Max Moment 10,000 kip-in

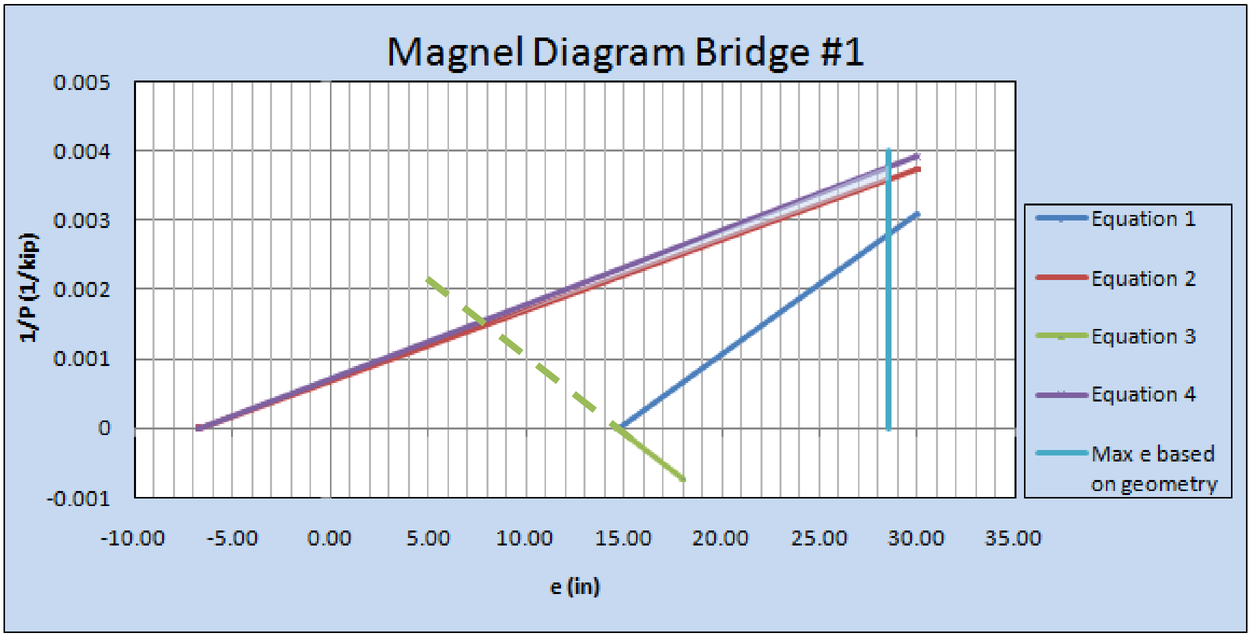

Figure D.14 (Bridge 1) 48.9% Max Moment (8750 kip-in)

APPENDIX E. SITE VISIT PHOTOGRAPHS

Bridge #1

Figure E.1 Bridge 1 Looking South

Figure E.2 Exposed Rebar on Bridge 1

Figure E.3 Bridge 1 T-girders and diaphragm

Bridge #2

Figure E.4 Bridge 2 - Railing and streambed

FigureE.5 Bridge 2 - Double T-beams

Figure E.6 Bridge 2

Figure E.7 Bridge 2 - Exposed Girder Flanges

Bridge #3

Figure E.8 Bridge 3 - span

Figure E.9 Bridge 3 **-** Underside of prestressed box girders

Bridge #4

Figure E.10 Deck of Bridge 4

Figure E.11 Bridge 4 **-** Double T-beams

Bridge #5

Figure E.12 Deck of Bridge 5

Figure E.13 Difficult access to underside of Bridge 5

Bridge #6

Figure E.14 Deck of Bridge 6

Figure E.15 Bridge 6 - Double T- Beams

Figure E.16 Spalling of concrete on Bridge 6

Bridge #7

Figure E.17 Deck of Bridge 7

Figure E.18 Bridge 7 **-** Concrete slab

Figure E.19 Bridge 7 **-** Underside of concrete slab

Bridge #8

Figure E.20 Deck of Bridge 8

Figure E.21 Bridge 8 **-** Span

Figure E.22 Bridge 8 **-** Slight arch in bridge girders

Figure E.23 Bridge 8 **-** Double T**-** girders and diaphragms

Figure E.24 Bridge 8 **-** Double T**-** girders and diaphragms

Figure E.25 Bridge 8 **-** Rust at supports

Bridge #9

Figure E.26 Deck of Bridge 9

Figure E.27 Bridge 9

Figure E.28 Bridge 9 - span

Figure E.30 Underside of Bridge 9

Bridge #10

Figure E.31 Diaphragm and double T-girder of Bridge 10

Figure E.32 Deck of Bridge 10

Figure E.33 Bridge 10 - Three spans

Figure E.34 Bridge 10 Double T- Girders

Figure E.35 Bridge 10 Pier

Bridge #11

Figure E.36 Bridge 11 Deck - Exposed Flange

Figure E.37 Bridge 11 Span

Figure E.38 Bridge 11 U-girders

Bridge #12

Figure E.39 Bridge 12 Double T-girders

Figure E.40 Bridge 12 **-** Exposed rebar at girder joint

Figure E.41 Bridge 12 Streambed

Figure E.42 Bridge 12 Double T-girders

Bridge #13

Figure E.43 Bridge 13 Deck

Figure E.44 Bridge 13 Downstream Screen

Bridge #14

Figure E.45 Bridge 14 Double T-girders

Figure E.46 Bridge 14 Deck

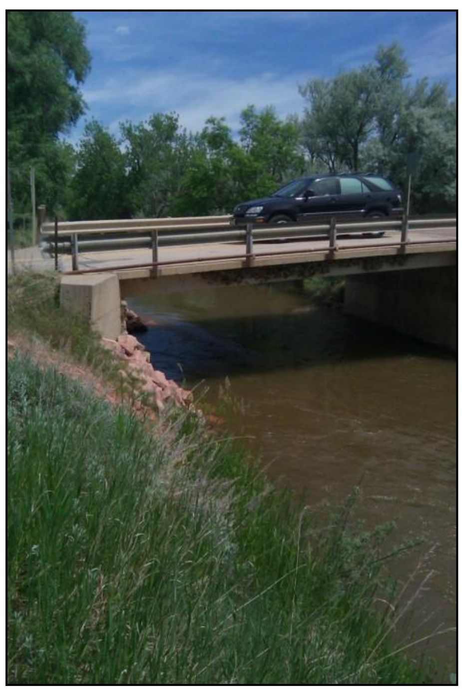

Figure E.47 Bridge 14 Span

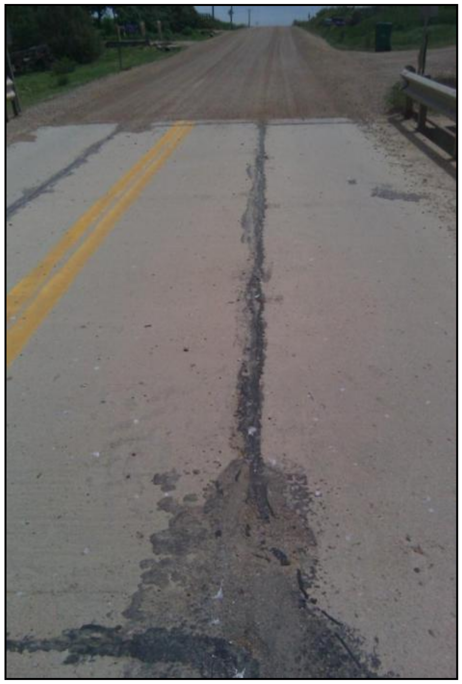

Figure E.48 Bridge 14 **-** Sealant on joints

Bridge #15

Figure E.49 Bridge 15 Deck

Figure E.50 Bridge 15 **-** Double T**-** girder and slab

Figure E.51 Bridge 15 **-** Exposed Rebar

FigureE.52 Bridge 15 Widened with Double T-Girder

Bridge #16

Figure E.53 Bridge 16 Double T- girders and diaphragm

Figure E.54 Bridge 16 Supports

Figure E.55 Bridge 16 - Exposed rebar on wearing surface

Figure E.56 Bridge 16 - Exposed Girder Flanges

Figure E.57 Bridge 16 - Wing wall and Girders

Figure E.58 Bridge 16 - Cracking at girder joint